

Multisensor Online Transfer Learning for 3D LiDAR-based Human Classification with a Mobile Robot

Zhi Yan¹, Li Sun², Tom Duckett², and Nicola Bellotto²

Abstract—Human detection and tracking is an essential task for service robots, where the combined use of multiple sensors has potential advantages that are yet to be exploited. In this paper, we introduce a framework allowing a robot to learn a new 3D LiDAR-based human classifier from other sensors over time, taking advantage of a multisensor tracking system. The main innovation is the use of different detectors for existing sensors (i.e. RGB-D camera, 2D LiDAR) to train, online, a new 3D LiDAR-based human classifier, exploiting a so-called trajectory probability. Our framework uses this probability to check whether new detections belongs to a human trajectory, estimated by different sensors and/or detectors, and to learn a human classifier in a semi-supervised fashion. The framework has been implemented and tested on a real-world dataset collected by a mobile robot. We present experiments illustrating that our system is able to effectively learn from different sensors and from the environment, and that the performance of the 3D LiDAR-based human classification improves with the number of sensors/detectors used.

I. INTRODUCTION

Human detection and tracking is an important task in service robotics, where knowledge of human motion properties such as position, velocity and direction can be used to improve the behavior of the robot, for example to improve its collision avoidance and adapt its velocity to that of the surrounding people.

Using multiple sensors to track people has advantages over a single one. The most obvious one is that multiple sensors can often do the task with a wider field of view and thus track more people within a larger range [1], [2]. Another advantage is that multiple sensors providing redundant information can increase tracking accuracy and reliability [3], [4]. Different sensors have different properties, including field of view. The 3D LiDAR in our robot platform (Fig. 1) has 16 scan channels, 360° horizontal and 30° vertical fields of view, and up to 100 m range. However, the measurement returned by this sensor are discrete points in space (i.e. point cloud), from which it is difficult to identify people because some low-level features, such as texture and colour, are missing. The 2D LiDAR has similar problems. The RGB-D camera, instead, can detect humans more reliably but only within a short range and small field of view (see Fig. 2).

We consider a particular problem in multisensor people tracking: there are different types of sensors, some of which already do have good human detectors, while other sensors

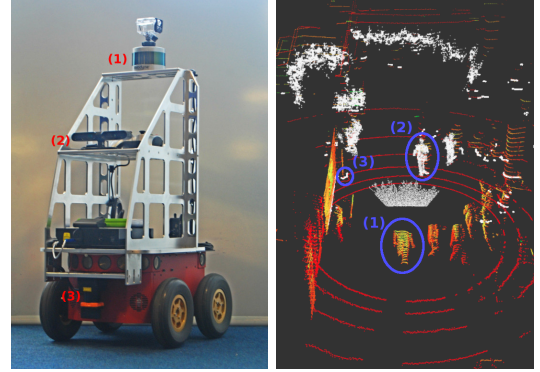


Fig. 1. Left: our robot platform including a Pioneer 3-AT mobile robot with four wheels for indoor use and a built-in odometry sensor, a Velodyne VLP-16 3D LiDAR (1), an ASUS Xtion PRO LIVE RGB-D camera (2), and a HOKUYO UTM-30LX 2D LiDAR (3). Right: visualized sensor data (only depth information is shown for RGB-D camera) annotated with corresponding sensor numbers.

do not. We wish the latter to learn such a detection ability from the existing sensors, and ultimately improve the overall performance of people tracking. In this paper we focus on the first part only and learn a classifier to distinguish between human and non-human 3D LiDAR detections, leaving the second part for future work.

Typically, data collection and training of the classifier are done offline, with obvious labour cost and potential human errors. With our new framework, instead, a 3D LiDAR-based human classifier is learned online using tracking information and pre-trained human detectors for 2D LiDAR and RGB-D sensors. In general, the framework allows a new sensor to learn from the trajectories of the tracking system, each one with an associated probability of being human-generated, and fusing both model-based (labeled) and model-free (unlabeled) detections from different detectors according to a semi-supervised learning scheme [5]. In contrast to previous approaches [6], [7], our solution does not need any hand-labeled data, performing online learning completely from scratch. This feature also makes our system easily adaptable to the environment where the robot is deployed.

The contributions of this paper are as follows: 1) we propose an online transfer learning framework for multisensor people tracking based on a *trajectory probability*, which takes into account both sensor independence in the detection and multisensor interaction in the trajectory estimation; 2) we present an experimental evaluation of our system for 3D LiDAR-based human classification with a mobile robot on a real-world dataset using different sensor combinations.

¹Laboratoire Electronique Informatique Image (Le2i), University of Technology of Belfort-Montbéliard (UTBM), France zhi.yan@utbm.fr

²Lincoln Centre for Autonomous Systems (L-CAS), University of Lincoln, UK {lsun, tduckett, nbellotto}@lincoln.ac.uk

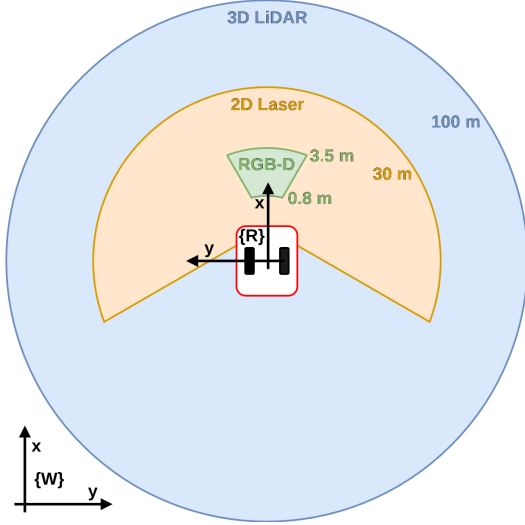


Fig. 2. Different horizontal fields of view of different sensors. Vertical fields of view, not shown in this figure, are also different.

The remainder of this paper is organized as follows: Section II gives an overview of the related literature. Section III formulates the problem in multisensor background. Section IV presents our solution framework for online transfer learning. Section V describes the application of the proposed framework to the problem of 3D LiDAR-based human classification. Section VI illustrates the experimental results for different sensor configurations. Finally, Section VII concludes the paper summarizing the contributions and suggesting future research work.

II. RELATED WORK

The problem of multitarget and multisensor tracking has been extensively studied during the past few decades. Most of present systems are based on Bayesian methods [8], which compute an estimate of the correspondence between features detected in the sensor data and the different humans to be tracked. Regarding robotic applications, multiple sensors can be deployed in single- or multi-robot systems [9], while the former is the concern of this paper.

RGB/RGB-D camera plus 2D LiDAR is the most frequently used combination in the literature. [3] presented two different methods for mobile robot tracking and following of a fast-moving person in an outdoor environment. The robot was equipped with an omnidirectional camera and a 2D LiDAR. [10] presented an integrated system to detect and track people and cars in outdoor scenarios, based on the information retrieved from a camera and a 2D LiDAR on an autonomous car. [2] introduced a people tracking system for mobile robots in very crowded and dynamic environments. Their system was evaluated with a robot equipped with two RGB-D cameras, a stereo camera and two 2D LiDARs.

Our previous work with the aforementioned sensor combination includes [11] and [12]. The former presented a human tracking system for mobile service robots in populated environments, while the latter extended this system to

a fully integrated perception pipeline for people detection and tracking in close vicinity to the robot. The proposed tracking system tracks people by detecting legs extracted from a 2D LiDAR and fusing this with the faces or the upper-bodies detected with a camera using a sequential implementation of the Unscented Kalman Filter (UKF).

The combination with 3D LiDAR is increasing with the development of the 3D LiDAR technology. Taking advantage of its high accuracy, [4] developed an algorithm to align 3D LiDAR data with high-resolution camera images obtained from five cameras, in order to accurately track moving vehicles. Other reported results include [13] and [14], which mainly focused on pedestrian detection rather than tracking. In addition, earlier work presented multitarget tracking with a mobile robot equipped with two 2D LiDARs, respectively located at the front and back [1]. Thus the robot can have a 360° horizontal field of view, where each scan of these two sensors covers the whole surrounding of the robot at an angular resolution of 1°.

The use of machine learning algorithms for tracking has particular advantages. The closest work to ours is [7], where the authors proposed a semi-supervised learning approach to the problem of track classification in 3D LiDAR data, based on Expectation-Maximization (EM) algorithm. In contrast to our approach, their learning procedure needs a small set of seed tracks and a large set of background tracks, that need to be manually or semi-manually labeled at first, whereas we do not need any hand-labeled data.

To our knowledge, no existing work in the robotics field exploits information from multisensor-based tracking to implement transfer learning between different sensors as in this paper. Our work combines the advantages of multiple sensors with the efficiency of semi-supervised learning, and integrates them into a single online framework applied to 3D LiDAR-based human classification.

III. PROBLEM FORMULATION

In this section, we model the problem of online learning for human classification in a multitarget-multisensor tracking system. The formulation is generalized which can be extended to objects rather than humans. We consider online learning as a *detection-and-tracking-based* iterative process. Whilst this idea has been presented in the computer vision literature [15], it has yet to be applied in robotics. In addition, we put the problem into a multisensor system context, which distinguishes this formulation from previous work.

We assume firstly that, in terms of hardware, a robot perceives the environment through a finite set S of sensors. Sensors $s_1, s_2, \dots, s_n \in S$ may have completely different perception mechanisms and may produce a variety of types of sensory data such as point clouds, laser scans, images, etc. We assume secondly that, in terms of software, the robot detects humans through a finite set D of detectors. Detectors $d_1, d_2, \dots, d_n \in D$ can be different. For example d_1 can be for human face detection, d_2 for legs, d_3 for whole body, etc. Moreover, $f : D \xrightarrow{1:1} S$ is not necessary, meaning that a sensor can have zero or several detectors, and a detector

can also be shared by several sensors. This statement is the base of the paper, making it possible for one sensor to learn from another.

We consider a multitarget-multisensor tracking system with K sensors and N human targets. The system is composed of two processes, detection and actual tracking (or state estimation). The detection process at time t can be modeled as a non-linear function \mathcal{F}_D :

$$P(y|Q_t) = \mathcal{F}_D(Q_t) \quad (1)$$

where the set of acquisitions (or observations)

$$Q_t = \{x_i^j, r_t\}_{i \in 1:N, j \in 1:K} \quad (2)$$

includes the sensor data x_i^j of the i th human from the j th sensor and the robot state r_t . $Y\{y_1, \dots, y_N\}$ is a set of human detections ground truth and for each y_i the category and the position information are given. The process of detection is to maximize the detection likelihood:

$$\mathcal{L}_D(X, Y) = \sum_{i \in 1:N} \sum_{j \in 1:K} f_L^d(x_i, y_i) \quad (3)$$

where f_L^d is the detection likelihood function.

Similarly, the tracking process can also be treated as a non-linear function \mathcal{F}_T :

$$P(Y_t|Q_t, Q_{t-1}, \dots) = \mathcal{F}_T(Q_t, Q_{t-1}, \dots) \quad (4)$$

and the tracking likelihood also need to be maximized:

$$\begin{aligned} \mathcal{L}_T(Y_t, \mathcal{F}_T(Q_t, Q_{t-1}, \dots)) \\ = \sum_{i \in 1:N_T} f_L^T(y_i^t, \mathcal{F}_D(Q_t), \mathcal{F}_D(Q_{t-1}), \dots) \end{aligned} \quad (5)$$

where N_T is the number of trajectories and f_L^T is the tracking likelihood function of a single trajectory.

We assume that detection x_i can be done with or without a label. Let $(Q_T, Y_T) = (< X_T, R_T >, Y_T) = \{(< x_1, r_1 >, y_1), \dots, (< x_t, r_t >, y_t)\}_T$ be all the data observed through time $T = \{1 : t\}$, where $y_i \in \mathbb{N}$ denotes the label with $y_i = 0$ for unlabeled data. The goal is to learn a classifier to predict the class label of each incoming detection, and then update the classifier based on the result obtained (x_i alone or (x_i, y_i)). For an online learning process, the halting criteria is significantly important. We define the learning stability function at iteration I as *stability_I*. Theoretically, the whole online learning process is stable if:

$$\lim_{I \rightarrow \infty} \frac{\text{stability}_I}{I} = 0 \quad (6)$$

One can halt the learning process when the stability stops increasing, or other stopping conditions (e.g. maximum iteration) are triggered.

IV. SOLUTION FRAMEWORK

An overview of our solution framework for online transfer learning can be seen in Fig. 3. It contains four main components: static detectors denoted by \mathcal{D}_s , dynamic detectors \mathcal{D}_d , a target tracker \mathcal{T} and a label generator \mathcal{G} . In order to facilitate the explanation, we present each component

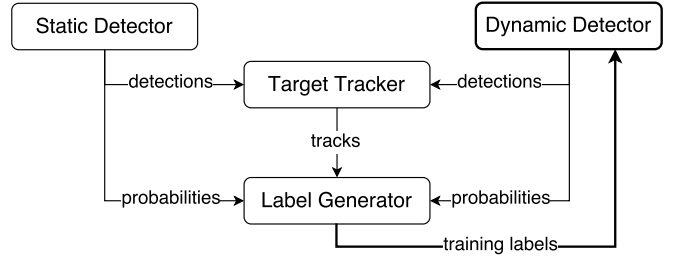


Fig. 3. Block diagram of the online transfer learning framework.

following the sequence of an entire iteration, starting with human detection. Moreover, to simplify the notation, the following discussion will consider only single class problems. The extension to multiclass is straightforward.

A. Human Detection

\mathcal{D}_s can detect humans with offline-trained or heuristic detectors, typically with high confidence, while \mathcal{D}_d acquires this ability through the online framework. Both detectors provide new observations for \mathcal{T} and their corresponding probabilities for \mathcal{G} . On one hand, \mathcal{D}_s enables category-specific tracking i.e. human tracking and, on the other, it helps the learning of \mathcal{D}_d , so that the latter can improve human detection and eventually human tracking. \mathcal{D}_s provides labeled detections, while \mathcal{D}_d provides both labeled and unlabeled ones. In our previous work [6], \mathcal{D}_d could be learnt without \mathcal{D}_s by providing a relatively small initial set of training samples and using a specific \mathcal{G} tailored for the type of data (i.e. 3D LiDAR clusters). Here we assume the initial training set is substituted, instead, by a transfer learning process between the initial \mathcal{D}_s and the final \mathcal{D}_d . In addition, \mathcal{G} is generalized to produce new samples independently from their particular data structure.

B. Target Tracking

The tracking process \mathcal{T} gathers the observations, fuses them and generates human motion estimates. Both moving and stationary targets are tracked. For the latter, the trajectory length is supposed to be null or at least very small. \mathcal{T} plays a key role in the whole framework, because it associates human detections from different sensors to the same corresponding estimates, linking \mathcal{D}_s and \mathcal{D}_d detections and therefore making the transfer learning possible. In order to enable this on a mobile robot with multiple sensors, \mathcal{T} should meet the following requirements:

- be robust to sensor noise and partial occlusions;
- fuse multisensor data;
- be able to deal with multiple targets simultaneously;
- cope with noise introduced by robot motion.

C. Transfer Learning

The label (or sample) generator \mathcal{G} fuses the information coming from \mathcal{D}_s , \mathcal{D}_d and \mathcal{T} , then generates training labels for \mathcal{D}_d . A *trajectory probability* is measured by \mathcal{G} , based on Bayes' theorem. The idea is to measure the likelihood that a track belongs to a human, which is defined as follow. Let

$P(y_i|x_i, d_j)$ denote the probability that sample (objectness proposal) x_i is a human observed by detector $d_j \in \mathcal{D}$, with $\mathcal{D} = \mathcal{D}_s \cup \mathcal{D}_d$, at time t . The probability of the whole track $P(Y_T|X_T, \mathcal{D})$, during the time interval T , is computed by integrating the observations of the different detectors according to the following formula:

$$P(Y_T|X_T, \mathcal{D}) = \frac{\text{odds}_{X_T}}{1 + \text{odds}_{X_T}} \quad (7)$$

where

$$\text{odds}_{X_T} = \prod_{i=1}^t \prod_{j=1}^K \text{odds}_{x_i}^j \quad (8)$$

and

$$\text{odds}_{x_i}^j = \frac{P(y_i|x_i, d_j)}{1 - P(y_i|x_i, d_j)} \quad (9)$$

An intuitive approach to generate labels is to threshold the trajectory probability in (7). Let σ be a predefined threshold value, then:

$$\begin{aligned} \forall (x_i, y_i) \in X_T \text{ assign } y_i = z (z \in \mathbb{Z}^+), \\ \text{if } P(Y_T|X_T, \mathcal{D}) \geq \sigma \end{aligned} \quad (10)$$

where \mathbb{Z}^+ refers to positive integer values. We propose to adopt a *batch-incremental training* policy to learn a classifier in \mathcal{D}_d , because: a) $|X_T| \geq 1$, and b) there are more choices of classifier and this approach adapts to concept drift for online learning [16]. For a certain interval, a new batch of training samples $[X_{new}, Y_{new}]$ can be generated:

$$\begin{aligned} [X_{new}, Y_{new}] = \{ (x_i, y_i) | x_i \in X_T \subseteq \mathbb{R}^n, \\ y_i \in Y_d \subseteq \mathbb{Z}^+, 1 \leq i \leq n_i \}_{\forall T} \end{aligned} \quad (11)$$

where X_T is obtained by tracker and Y_d is obtained by detectors. Let h_i denote the classifier trained on i th iteration, then the Batch Incremental Training (*BIT*) procedure can be defined as:

$$\mathcal{D}_d^i = \text{BIT}([X_{new}, Y_{new}], \mathcal{D}_d^{i-1}) \quad (12)$$

where subscript i refers to the iteration rather than time.

In summary, it can be seen that our solution is in fact an online semi-supervised learning framework, which: a) learns non-iid $P(X_i)$ sequentially, but fully labeled by \mathcal{G} ; b) learns from both labeled and unlabeled data, but in batch mode. The learning procedure converges when the number of correct detections output by \mathcal{D}_d reaches a steady state as shown in Equation 6. In this paper, we defined the stability at the iteration I as:

$$\begin{aligned} \text{stability}_I = \sum_{i=1}^I \| \sum_{N_i} y_i \cap \Lambda(P(y|Q_d^i, \mathcal{D}_d^i)) \\ - \sum_{N_{i+1}} y_{i+1} \cap \Lambda(P(y|Q_d^{i+1}, \mathcal{D}_d^{i+1})) \| \end{aligned} \quad (13)$$

where Λ is a binary function via thresholding σ .

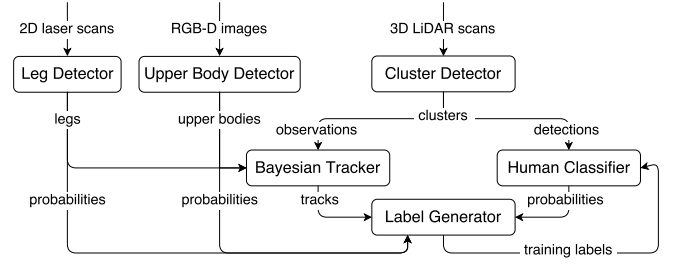


Fig. 4. Process details of the online transfer learning for human detection.

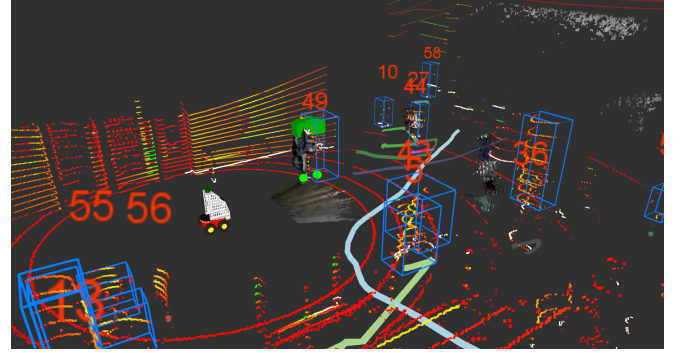


Fig. 5. A screenshot of our multisensor-based detection and tracking system in action. The sparse colored dots represent the laser beams with reflected intensity from the 3D LiDAR. The white dots indicate the laser beams from the 2D LiDAR. The non-rigid images is XYZ-RGB point cloud combined RGB image and Depth image from the RGB-D camera. The robot is at the center of the 3D LiDAR beam rings. The numbers are the tracking IDs and the colored lines represent the people trajectories generated by the tracker. For example, the man with tracking ID 49 has been detected by the upper-body detector (green cube), the leg detector (green circle), and the cluster detector (blue bounding box).

V. CASE STUDY

In this section, we present an online transfer learning for human classification in 3D LiDAR scans as a case study. It serves as a specific instantiation of the general framework presented, with which we can test our solution in a real robotic system (see Fig. 1). The detailed block diagram of our implementation can be seen in Fig. 4. At each iteration, 3D LiDAR scans are first segmented into point clusters. The position and velocity of these clusters are estimated in two-dimensional space in real-time by a multitarget tracking system, which outputs the tracks of all the clusters. At the same time, a classifier predicts the probabilities that the clusters are human. The classifier is initialized and retrained online. The tracks and the probabilities are output to a label generator, while the latter generates the training labels for the next iteration. The upper-body detector and the leg detector with their offline trained classifiers serve as static detectors. Both can improve the human tracking by sending the position of the detections on one hand, and providing the corresponding probabilities to the label generator on the other. For an intuitive understanding, please refer to Fig 5. The following paragraphs describe each module in detail.

A. \mathcal{D}_s : Upper Body Detector and Leg Detector

The upper-body detector [17] identifies upper-bodies (i.e. shoulders and head) in RGB-D images, taking advantage of a template and the depth information of the RGB-D camera. The leg detector [18] detects legs in 2D LiDAR scans based on 14 features, including the number of beams, circularity, radius, mean curvature, mean speed, and more.

B. \mathcal{D}_d : Cluster Detector and Human Classifier

As input of this module, a 3D LiDAR scan is defined as a set of points (i.e. a 3D point cloud):

$$P = \{p_i | p_i = (p_x^i, p_y^i, p_z^i) \in \mathbb{R}^3, i = 1, \dots, N_p\} \quad (14)$$

Clusters are extracted from point cloud P , based on the Euclidean distance between points in 3D space. A cluster can then be defined as follows:

$$X : \{x_i\} \subset P, i = 1, \dots, N_x \quad (15)$$

where N_x is the total number of clusters. A condition to avoid overlapping clusters is that they should not contain the same points, that is:

$$x_i \cap x_j = \emptyset, \text{ for } i \neq j, \text{ if } \min\|p_i - p_j\|_2 \geq d \quad (16)$$

where the sets of points $p_i, p_j \in P$ belong to the point clusters x_i and x_j , respectively, if the minimum distance between p_i and p_j is greater than or equal to a given distance threshold d . For more implementation details, please refer to [6].

Six features (a total of 61 dimensions) are extracted from the clusters for human classification, as shown in Table I. The set of feature values of each sample x_i forms a vector $f_i = (f_1, \dots, f_6)$. Features from f_1 to f_4 were introduced by [19], while features f_5 and f_6 were proposed by [20]. A Support Vector Machine (SVM) [21] is used to train the human classifier, because of its effectiveness on non-linear classification, and it has been experimentally proved to be efficient in 3D LiDAR-based human detection [20], [19]. A binary classifier (i.e. human or non-human) is trained at each iteration, based on the above features, using LIBSVM [22]. The ratio of positive to negative training samples is set to 1 : 1, and all data are scaled to $[-1, 1]$, generating probability outputs and using a Gaussian Radial Basis Function kernel [23]. Since LIBSVM does not currently support incremental learning, the system stores all the training samples accumulated from the beginning and retrains the entire classifier at each new iteration. The solution framework, however, also allows for other classifiers and learning algorithms.

C. \mathcal{T} : Bayesian Tracker

Cluster tracking is performed by a robust Bayesian estimator. The estimation consisting of two steps. In the first step, the following constant velocity model is used to predict the target state at time t given the previous state at $t - 1$:

$$\begin{cases} x_k = x_{k-1} + \Delta t \dot{x}_{k-1} \\ \dot{x}_k = \dot{x}_{k-1} \\ y_k = y_{k-1} + \Delta t \dot{y}_{k-1} \\ \dot{y}_k = \dot{y}_{k-1} \end{cases} \quad (17)$$

TABLE I
FEATURES FOR HUMAN CLASSIFICATION

Feature	Description	Dimension
f_1	Number of points included in the cluster	1
f_2	Minimum cluster's distance from the sensor	1
f_3	3D covariance matrix of the cluster	6
f_4	Normalized moment of inertia tensor	6
f_5	Slice feature for the cluster	20
f_6	Reflection intensity's distribution	27

where x and y are the position of a tracking target in the two-dimensional Cartesian coordinates, \dot{x} and \dot{y} are the respective velocities, and Δt is the time difference between t and $t - 1$.

In the second step, if one or more new observations are available from the detectors, the predicted states are updated using a Cartesian or a Polar observation model, depending on the type of sensor:

$$\begin{cases} \mu_k = x_k \\ \nu_k = y_k \end{cases} \quad \text{or} \quad \begin{cases} \theta_k = \tan^{-1}(y_k/x_k) \\ \gamma_k = \sqrt{x_k^2 + y_k^2} \end{cases} \quad (18)$$

where (μ, ν) and (θ, γ) are the Cartesian and the Polar coordinates, respectively, from the detectors. For more implementation details, please refer to [24].

D. \mathcal{G} : Label Generator

The positive training labels X^+ are generated according to Equation 10, while the negatives X^- are generated based on a volume filter:

$$X^- = \{x_i \mid W_i < 0.2, W_i > 1.0, D_i < 0.2, D_i > 1.0, H_i < 0.2, H_i > 2.0\} \quad (19)$$

where W_i, D_i, H_i are the width, depth and height of a 3D cluster x_i . The idea is that clusters without a pre-defined human-like volumetric model will be considered as negative samples for the next training iteration.

VI. EVALUATION

A. Dataset

We evaluated our framework on a real-world dataset¹ collected, in an indoor public area in our university, by the robotic platform shown in Fig. 1. The robot was running on the Robot Operating System (ROS) [25], and its navigation was controlled with a gamepad by hand. The ground truth was recorded into several *rosbag* files. The total length of the recorded data is about 49 minutes, including 19 and 30 minutes segments of *continuous* ground truth. The recorded ROS topics and the corresponding specifications are summarized in Table II. Sensor data were recorded in their original frame of reference and the transformation between the coordinate frames is implemented by the ROS *tf* package.

¹<https://lcas.lincoln.ac.uk/wp/research/data-sets-software/l-cas-multisensor-people-dataset/>

TABLE II
RECORDED ROS TOPICS IN A ROSBAG FILE

Topic (<i>message type</i>)	Description	Frequency
camera/depth/image_raw (<i>sensor_msgs/Image</i>)	Depth image from the RGB-D camera	30 Hz (18 MB/s)
scan (<i>sensor_msgs/LaserScan</i>)	Scan data from the 2D LiDAR	40 Hz (120 KB/s)
velodyne_packets (<i>velodyne_msgs/VelodyneScan</i>)	Scan data from the 3D LiDAR	10 Hz (1 MB/s)
pose (<i>nav_msgs/Odometry</i>)	Odometry data from the robot	10 Hz (7 KB/s)

B. Experimental Setup

The experiments were conducted on the 19 minutes segment of continuous data, in which a binary SVM for human classification was learned online. The classifier was retrained once every 300 new positive (human) and 300 new negative (non-human) samples, corresponding to one iteration. We report the results for the first seven iterations, collecting a total of 2,100 positive and 2,100 negative. In addition, a classifier was trained offline, using 2,100 manually labeled positive samples with an equal amount of randomly selected negative samples, to serve as a baseline for comparison.

We arbitrarily selected 100 scan frames from the dataset and fully annotated these (including standing and sitting people) as a test set. This contains 1,197 human labels with distance from the 3D LiDAR between 0.02 m and 22.5 m. A true positive was considered if the overlap between the ground truth and the detection was larger than 50%. Our framework has been fully implemented into ROS with high modularity. All components are ready for download² and use by other researchers. The dataset collection, as well as all the experiments reported in this paper, were carried out with an Intel i7-4785T processor and 8 GB memory, using Linux Ubuntu 14.04 LTS (64-bit) and ROS Indigo.

C. Human Classification

In this section, we evaluate the performance of the 3D LiDAR-based human classification after every online training iteration. We compare human classification performance for all possible combinations of sensors: 3D LiDAR only, learning by itself without any knowledge transfer, similar to [6]; 3D LiDAR with RGB-D camera; 3D LiDAR with 2D LiDAR only; 3D LiDAR with both RGB-D camera and 2D LiDAR. We measure the average precision (AP) [26] rather than the classification accuracy (ACC) used in [7]. This is because in our binary classification the true negatives were far more common than the true positives, making the ACC always higher than 80% in each training iteration for all combinations (with probability threshold set to 0.5). In all experiments, the trajectory probability threshold σ of (10) was set to 0.7.

The experimental results are shown in Fig. 6. The overall trends of AP for “3D LiDAR only” and “with 2D LiDAR”

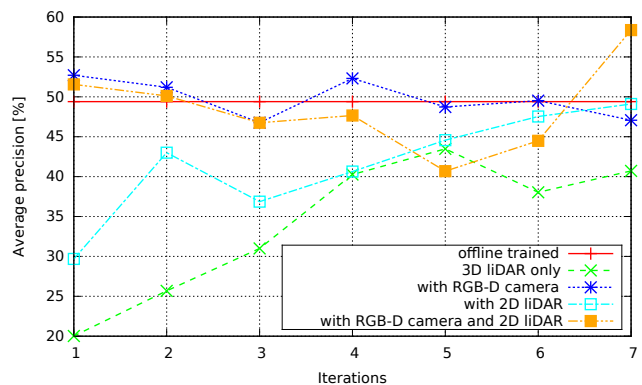


Fig. 6. Human detection performance comparison taking the offline trained classifier as a baseline.

rise with the iterations, while that of “with RGB-D camera” declines. This is because the RGB-D camera was mounted on our robot at 0.55 m from the floor, which is relatively low for human upper-body detection in close vicinity to the sensor. The confidence of the upper-body detector is inversely proportional to the observation range, affecting the learning of the new classifier. However, the results of “with RGB-D camera and 2D LiDAR” show an interesting curve, first dropping until iteration 5, and then rising. This actually shows the advantage of multisensor systems, which can overcome individual sensor biases.

We additionally evaluate the offline and online trained final classifiers (i.e. after the 7th iteration) using the Precision-Recall metric. The experimental results are shown in Fig. 7. Once again, the combination of RGB-D camera and 2D LiDAR shows a better performance. In contrast to the “3D LiDAR only” case, which only learned from moving people, the “with RGB-D camera and 2D LiDAR” case was able to learn from moving, standing and sitting people, greatly improving the human classification performance. It is also worth pointing out that the offline trained classifier shows a relatively high precision but the true positive rate (recall) is much lower. This is due to a lack of long-distance samples in the offline training set, which are difficult to label by a human annotator.

VII. CONCLUSION

In this paper, we presented a framework for online transfer learning, applied to 3D LiDAR-based human classification, taking advantage of multisensor-based tracking. The framework, which relies on the computation of human trajectory probabilities, enables a robot to learn a new human classifier over time with the help of existing human detectors. To this end, we proposed a semi-supervised learning method, which fuses both model-based (labeled) and model-free (unlabeled) detections from different sensors. A very promising feature of the proposed solution is that the new human classifier can be learned directly from the deployment environment, thus removing the dependence on pre-annotated data. The experimental results, based on a real-world dataset, demonstrated the efficiency of our system.

²https://github.com/LCAS/online_learning/tree/multisensor

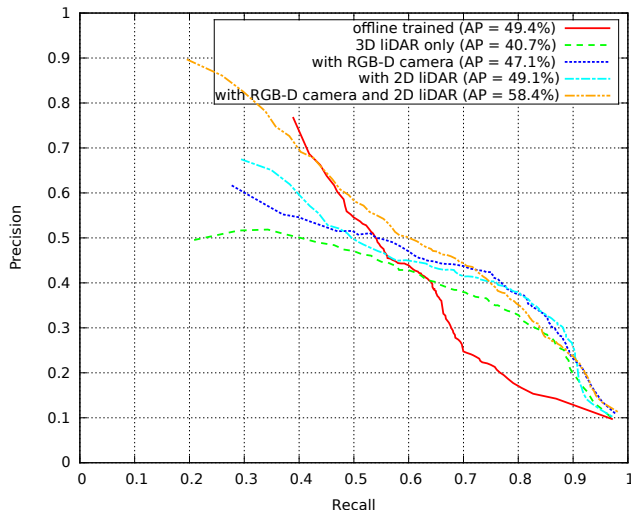


Fig. 7. Performance evaluation of human detection.

The proposed framework has been fully implemented into ROS with a high level of modularity. The software and the dataset are publicly available to the research community, with the intention to perform objective and systematic comparisons between the recognition capabilities of different robots. Moreover, our framework is easy to extend to other sensors and moving objects, such as cars, bicycles and animals.

Despite these encouraging results, there are several aspects which could be improved. For example, the AP of the online learned classifier is still relatively low, due to the complexity of the environment recorded in our dataset. This can be further improved by using a more advanced model for negative sample generation, instead of relying on the simple volume filter in (19). In addition, it remains to be verified how a new human detector, based on the online trained classifier, will affect the stability of the system and its tracking performance.

ACKNOWLEDGMENT

This project has received funding from the European Union's Horizon 2020 research and innovation programme under grant agreement No 645376 (FLOBOT). Website: <http://www.flobot.eu/>

REFERENCES

- [1] D. Schulz, W. Burgard, D. Fox, and A. B. Cremers, "People tracking with mobile robots using sample-based joint probabilistic data association filters," *International Journal of Robotics Research*, vol. 22, no. 2, pp. 99–116, 2003.
- [2] T. Linder, S. Breuers, B. Leibe, and K. O. Arras, "On multi-modal people tracking from mobile platforms in very crowded and dynamic environments," in *Proceedings of the 2016 IEEE International Conference on Robotics and Automation (ICRA)*, 2016, pp. 5512–5519.
- [3] M. Kobilarov, G. Sukhatme, J. Hyams, and P. Batavia, "People tracking and following with mobile robot using an omnidirectional camera and a laser," in *Proceedings of the 2006 IEEE International Conference on Robotics and Automation (ICRA)*, 2006, pp. 557–562.
- [4] D. Held, J. Levinson, and S. Thrun, "Precision tracking with sparse 3d and dense color 2d data," in *Proceedings of the 20013 IEEE International Conference on Robotics and Automation (ICRA)*, 2013, pp. 1138–1145.

- [5] X. Zhu and A. B. Goldberg, *Introduction to Semi-Supervised Learning*. Morgan & Claypool, 2009.
- [6] Z. Yan, T. Duckett, and N. Bellotto, "Online learning for human classification in 3d lidar-based tracking," in *In Proceedings of the 2017 IEEE/RSJ International Conference on Intelligent Robots and Systems (IROS)*, 2017.
- [7] A. Teichman and S. Thrun, "Tracking-based semi-supervised learning," in *Proceedings of Robotics: Science and Systems*, 2011.
- [8] Y. Bar-Shalom and X.-R. Li, *Multitarget-multisensor tracking: principles and techniques*. Storrs, CT: University of Connecticut, 1995.
- [9] Z. Yan, N. Jouandeau, and A. Ali Cherif, "A survey and analysis of multi-robot coordination," *International Journal of Advanced Robotic Systems*, vol. 10, no. 399, December 2013.
- [10] L. Spinello, R. Triebel, and R. Siegwart, "Multiclass multimodal detection and tracking in urban environments," *International Journal of Robotics Research*, vol. 29, no. 2, pp. 1498–1515, 2010.
- [11] N. Bellotto and H. Hu, "Multisensor-based human detection and tracking for mobile service robots," *IEEE Transactions on Systems, Man, and Cybernetics – Part B*, vol. 39, no. 1, pp. 167–181, 2009.
- [12] C. Dondrup, N. Bellotto, F. Jovan, and M. Hanheide, "Real-time multisensor people tracking for human-robot spatial interaction," in *ICRA Workshop on Machine Learning for Social Robotics*, 2015.
- [13] C. Premebida, J. Carreira, J. Batista, and U. Nunes, "Pedestrian detection combining RGB and dense LIDAR data," in *Proceedings of the 2014 IEEE/RSJ International Conference on Intelligent Robots and Systems (IROS)*, 2014, pp. 4112–4117.
- [14] A. González, G. Villalonga, J. Xu, D. Vázquez, J. Amores, and A. M. López, "Multiview random forest of local experts combining RGB and LIDAR data for pedestrian detection," in *Proceedings of the 2015 IEEE Intelligent Vehicles Symposium (IV)*, 2015, pp. 356–361.
- [15] Z. Kalal, K. Mikolajczyk, and J. Matas, "Tracking-Learning-Detection," *IEEE Transactions on Pattern Analysis and Machine Intelligence*, vol. 34, pp. 1409–1422, 2012.
- [16] J. Read, A. Bifet, B. Pfahringer, and G. Holmes, "Batch-incremental versus instance-incremental learning in dynamic and evolving data," in *Proceedings of the Eleventh International Symposium on Intelligent Data Analysis (IDA 2012)*, 2012, pp. 313–323.
- [17] O. H. Jafari, D. Mitzel, and B. Leibe, "Real-time RGB-D based people detection and tracking for mobile robots and head-worn cameras," in *Proceedings of the 2014 IEEE International Conference on Robotics and Automation (ICRA)*, 2014, pp. 5636–5643.
- [18] K. O. Arras, O. M. Mozos, and W. Burgard, "Using boosted features for the detection of people in 2d range data," in *Proceedings of the 2007 IEEE International Conference on Robotics and Automation (ICRA)*, 2007, pp. 3402–3407.
- [19] L. E. Navarro-Serment, C. Mertz, and M. Hebert, "Pedestrian detection and tracking using three-dimensional lidar data," in *Proceedings of the 7th Conference on Field and Service Robotics (FSR)*, 2009, pp. 103–112.
- [20] K. Kidono, T. Miyasaka, A. Watanabe, T. Naito, and J. Miura, "Pedestrian recognition using high-definition LIDAR," in *Proceedings of the 2011 IEEE Intelligent Vehicles Symposium (IV)*, 2011, pp. 405–410.
- [21] C. Cortes and V. Vapnik, "Support-vector networks," *Machine Learning*, vol. 20, no. 3, pp. 273–297, 1995.
- [22] C.-C. Chang and C.-J. Lin, "LIBSVM: A library for support vector machines," *ACM Transactions on Intelligent Systems and Technology*, vol. 2, pp. 1–27, 2011, software available at <http://www.csie.ntu.edu.tw/~cjlin/libsvm>.
- [23] S. S. Keerthi and C.-J. Lin, "Asymptotic behaviors of support vector machines with gaussian kernel," *Neural Computation*, vol. 15, no. 7, pp. 1667–1689, 2003.
- [24] N. Bellotto and H. Hu, "Computationally efficient solutions for tracking people with a mobile robot: an experimental evaluation of bayesian filters," *Autonomous Robots*, vol. 28, pp. 425–438, 2010, software available at <https://github.com/LCAS/bayestracking>.
- [25] M. Quigley, K. Conley, B. P. Gerkey, J. Faust, T. Foote, J. Leibs, R. Wheeler, and A. Y. Ng, "ROS: an open-source robot operating system," in *ICRA Workshop on Open Source Software*, 2009.
- [26] M. Everingham, L. J. V. Gool, C. K. I. Williams, J. M. Winn, and A. Zisserman, "The pascal visual object classes (VOC) challenge," *International Journal of Computer Vision*, vol. 88, pp. 303–338, 2010.